DOI: 10.61782/fa.2025.0261

DEEP LEARNING-AIDED DESIGN OF A BROADBAND LOW-FREQUENCY META-ABSORBER FOR ROOM ACOUSTIC APPLICATIONS

Oluwaseyi Ogun[1] **John Kennedy**[1*]
[1] School of Engineering, Trinity College Dublin, Ireland, D02 PN40

ABSTRACT

Designing acoustic metamaterials (AMMs) capable of achieving broadband low-frequency absorption remains a considerable challenge due to the physical limitations imposed by long wavelengths, which typically necessitate thick, voluminous structures. This paper introduces a data-driven approach that employs a pretrained deep learning (DL) model to generate optimized AMM geometries based on targeted absorption spectra, which are tailored to room-specific modal behavior and layout. The resulting designs aim to maximize absorption efficiency within the 100–250 [Hz] range while minimizing structural footprint and material usage. The proposed AMM absorbers are evaluated through finite element simulations and validated against experimental reverberation time (RT60) measurements in a partially evacuated office environment. Performance is benchmarked against a commercial 10 [cm] thick Spektra A10 absorber. Results reveal that the AMM, with only 3 [cm] thickness, achieves competitive performance in the targeted low-frequency range, offering moderate RT60 reduction. While the Spektra A10 exhibits better performance above 200 [Hz], the AMM's compact form factor and design flexibility provide compelling advantages for low-frequency room treatment. These results highlight the potential of integrating machine learning with acoustic design to develop lightweight, application-specific absorption solutions for modern architectural acoustics.

**Corresponding author*: *jkenned5@tcd.ie.*

Keywords: *broadband absorption, deep learning, room acoustics, low-frequency.*

1. INTRODUCTION

The way sound is perceived within a room results from both direct sound—traveling straight from the source to the listener—and reflected sound, which bounces off various surfaces. Key contributors to these reflections include architectural features such as walls, floors, and ceilings, but other objects, including furniture and even people, can also influence sound propagation. How sound interacts with a surface depends on factors such as the material composition and the angle at which the sound wave strikes it. The acoustical analysis of a room is essential for understanding and optimizing the behavior of sound within enclosed spaces for optimal sound experience. The interaction of sound waves with surfaces, objects, and air affects how sound is perceived, making room acoustics a critical factor in designing environments such as concert halls, theaters, recording studios, classrooms, offices, and residential spaces [1]. Poor acoustic design can lead to issues such as excessive reverberation, speech intelligibility problems, and unwanted echoes, which degrade the quality of auditory experiences.

However, achieving a universally ideal acoustic environment for concerts and theaters for instance, is an idealization, as musical perception is influenced not only by objective sound characteristics, but also by individual perceptions and requirements. This inherent diversity in acoustic preferences leads to a wide range of successful concert hall designs, making room acoustics a continuously evolving field [2]. To navigate these complexities, acoustic modeling provides a structured approach to evaluate key sound characteristics within a space, and enables auralization [3].

The two primary methods for modeling room acoustics are based either on solving the Helmholtz wave equation or its variants, or on the principles of geometrical acoustics which form the foundation of ray acoustics. Geometrical acoustics, a commonly used approach for room acoustic modeling [1, 4–6], treats sound propagation as rays and disregards its wave nature. This assumption is accurate at high frequencies where the sound wavelength is much smaller than the objects and room features (e.g., walls, furniture). However, at low frequencies, wave phenomena such as diffraction and interference become more pronounced, leading to significant small-scale effects that geometrical acoustics cannot account for, thus necessitating wave-based methods such as the finite element modeling (FEM) or a hybrid approach [7].

Konrad et al. [8] explores simulating room acoustics using the finite-difference time-domain (FDTD) method, focusing on boundary and medium modeling. Their findings suggest that the proposed 3D schemes outperform traditional methods like Yee's staggered grid [9], and the digital waveguide mesh while maintaining desirable boundary properties. Elzbieta et al. [10] explores the theoretical and practical approaches to optimizing the sound field through architectural design. The study provides guidelines for acoustic planning, focusing on sound absorption strategies, spatial and material solutions, aiding systems, and proper device implementation. Noting a gap between acoustics and architecture, the paper bridges these fields by highlighting their mutual influence on sound absorption and propagation in office spaces.

Noise control in open offices can be achieved through high room absorption, tall screens, bookcases, and sufficient masking sound. However, the interaction of these elements is complex, particularly at varying distances from a speaker. Jukka et al. [11] conducted room acoustic measurements in 15 open offices and developed a model using multivariable regression analysis of the measurement data. Their model predicts two key descriptors of open office acoustics: the A-weighted speech level per distance doubling and the radius of distraction. These predictions are then used for decision making, to improve speech privacy and overall acoustic conditions.

An optimization model to help office space designers select cost-effective noise control materials while meeting acoustic quality requirements was presented in Abdullah et al. [12]. The model follows five key stages: identifying designer decisions affecting cost, formulating an optimization function, defining constraints related to acoustic quality and material selection, implementing the model using genetic algorithms (GA), and evaluating its performance in a real-world office space. Their model determines the optimal type and area of acoustic materials for each surface in the room, ensuring both cost efficiency and acoustic performance.

Low-frequency noise is still a challenge that is practically difficult to deal with especially in communication spaces where sound quality is non-trivial. Fuchs et al. [13] highlights the often-overlooked issue of low-frequency noise (below 100–125 [Hz]) in communication spaces such as offices, conference rooms, and restaurants. Traditional building and room acoustic standards fail to address this frequency range, which significantly impacts speech intelligibility and sound quality. To tackle this, the development and consulting institute, IBP, developed slender compound panel absorbers (CPA), which can be mounted on walls or ceilings to dampen dominant room eigenfrequencies. Through extensive real-world testing, the study demonstrates substantial improvements in acoustic comfort. The paper serves as a call to recognize the limitations of conventional acoustic ratings and proactively address low-frequency issues rather than waiting for updated standards.

Artificial intelligence (AI) has emerged as a transformative tool in the field of acoustics, revolutionizing acoustic design by enabling advanced noise control solutions. With its ability to analyze vast amounts of data and predict sound behavior with high precision, AI allows for the creation of customized acoustic environments tailored to specific needs, empowering designers to achieve targeted sound control with greater efficiency, and achieving optimized acoustics in spaces ranging from open offices to concert halls, while reducing time and resources spent on traditional trial-and-error approaches. A machine learning-based approach to estimate room acoustic parameters using only geometrical information as input was employed in [14]. The work demonstrates that traditional methods often rely on geometrical models (which approximate high-frequency sound as rays but lack accuracy for wave effects) or wave-based models (which are more precise but computationally expensive). The study builds a dataset from real-world acoustical measurements, using microphone array encoding to extract room impulse responses and absorption area in multiple directions. A neural network model is then trained to predict key acoustic parameters like reverberation time (T60) and early decay time (EDT). Compared to the traditional Sabine method, the model achieves higher accuracy, particularly at low frequencies.

In Ciaburro et al. [15], an automatic procedure for estimating the reverberation time of a room using artificial neural networks (ANNs) was developed. Traditionally, reverberation time measurement requires specialized equipment and exclusive access to the space. In contrast, their work proposed a method that uses simple audio recordings, from which acoustic features are extracted and labeled with corresponding reverberation time values in octave bands. The labeled dataset is then used to train an ANN model, enabling it to predict reverberation time in any closed space without the need for complex measurements or calculations. The approach simplifies and streamlines the process of estimating reverberation time, making it more accessible and efficient.

Low-frequency broadband noise is a common phenomenon in room acoustics, which is a challenge for traditional acoustic panels as they would need to be impractically bulky to absorb such frequencies. In this paper, a partially empty office space is considered for acoustic treatment. A wave-based numerical method based in COMSOL® Multiphysics is used to simulate the behavior of the room to sound, and the reverberation time measurements are compared with those from experiment. Next, a previously trained deep learning model of an acoustic metamaterial (AMM) absorber is used to predict broadband absorber geometries, with a user-specified subwavelength thickness, according to the experimentally determined room modes. This paper is structured as follows. Section 2 outlines the methodology, including the numerical modeling procedure, experimental setup, and the measurement metrics employed. Section 3 presents the results of the study, covering the validation of the numerical model and the performance comparison between the proposed AMM and a commercial-grade absorber based on RT60. Finally, Section 4 provides the conclusions and discusses key findings and potential improvements.

2. METHODOLOGY

2.1 Room description and numerical modeling

The considered office space is a rectangular room of dimensions 580 [cm] $\times$ 266 [cm] $\times$ 280 [cm], with a window of dimensions 130 [cm] $\times$ 54 [cm] $\times$ 180 [cm] as depicted in Fig. 1(a). The office is constructed with solid concrete and brick surfaces with reflective acoustic characteristics. The walls are made of exposed bricks, offering high mass and rigidity. This results in strong sound reflection, with minimal sound absorption at lower frequencies. The surface texture of the brick may introduce some diffusion at mid-to-high frequencies. The ceiling consists of a solid reinforced concrete slab, providing a highly reflective surface that contributes to sound reverberation within the room. The lack of absorption may lead to longer decay times for higher frequencies unless treated with acoustic materials. The floor is a polished concrete surface, which is both acoustically reflective and structurally robust. The smooth finish enhances high-frequency reflections, potentially increasing room brightness. The window is a rectangular opening with a shallow cavity ending in the glass backing. The glass pane, set at the rear of the cavity, influences both sound reflection and absorption characteristics.

The acoustic response of the room is modeled using the lossless Helmholtz wave equation within the Pressure Acoustics Module of COMSOL® Multiphysics. The medium is excited with a monopole domain source, applied through a spherical volumetric source. This configuration approximates an omnidirectional point source, which is representative of a typical loudspeaker or sound source in enclosed spaces. The spherical region ensures uniform radiation of acoustic energy in all directions, minimizing directional bias and better simulating diffuse field conditions assumed in statistical models such as the Sabine and Eyring formulas.

Boundary conditions are assigned to the room surfaces and furniture based on their respective material properties, as detailed in Tab. 1, and their absorptivities across octave band center frequencies are obtained from the literature [16, 17]. The computational domain is discretized using a tetrahedral mesh, with a maximum element size of $\lambda/7$, where λ represents the wavelength corresponding to the highest frequency of interest.

2.2 Reverberation time

Reverberation is a key acoustic parameter that defines how sound persists in a room after the source has stopped [18]. It significantly impacts both speech intelligibility and musical quality. Excessive reverberation can blur speech by masking short consonant sounds, while insufficient reverberation can make music sound lifeless and lacking in richness. The reverberation time, $RT60$, is the duration required for the sound level to decay by 60 dB after the source ceases. This metric provides insight into the room's acoustic properties and can be measured empirically by analyzing the sound pressure level over time. The RT60 in frequency domain is commonly computed

Table 1: Absorption coefficients of the surface materials in the investigated office space.

Surface		Absorptivities in Octave Bands					
Type	Material	125 [Hz]	250 [Hz]	500 [Hz]	1000 [Hz]	2000 [Hz]	4000 [Hz]
Window	Glass	0.18	0.06	0.04	0.03	0.02	0.02
Window frame	Plywood	0.28	0.22	0.17	0.09	0.1	0.11
Ceiling/floor	Concrete	0.01	0.01	0.015	0.02	0.02	0.02
Door	Wood	0.1	0.07	0.05	0.04	0.04	0.04
Side walls	Brick	0.03	0.03	0.03	0.04	0.05	0.07
Table	Wood	0.15	0.11	0.10	0.07	0.06	0.07

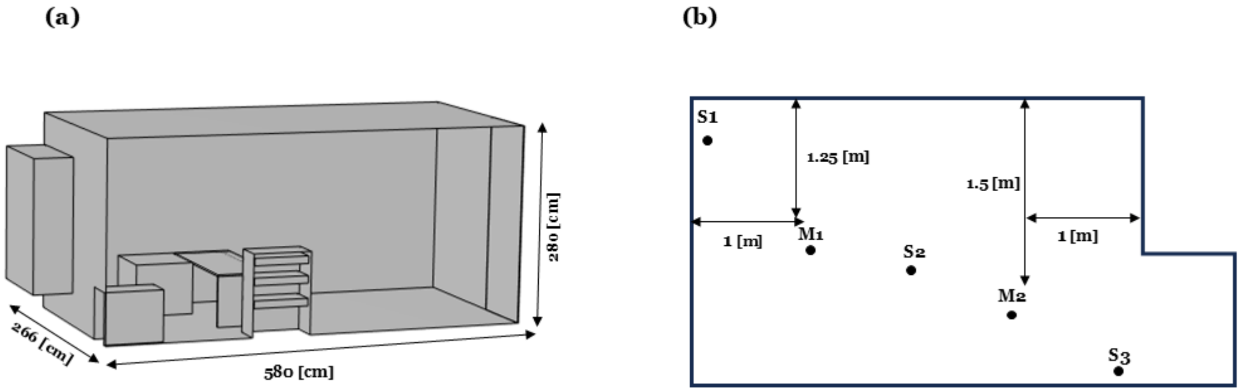

Figure 1: Illustration of the office space drawing simulated in COMSOL. (a) shows the CAD drawing of the room with a table, book shelve and a drawer, and (b) shows the map of the speaker-microphone positions during measurements.

according to the Sabine formula [19] in Eqn. (1)

$$RT60 = \frac{0.161V}{A}, \tag{1}$$

where V is the volume of the room, and A is the total equivalent absorption area given by

$$A = \sum (S_i.\alpha_i), \tag{2}$$

where S_i is the effective surface area of each material in the room, and α_i is the absorption coefficient of the material. The Sabine formula assumes that sound energy is uniformly distributed within the room, with minimal influence from objects and furniture on the overall acoustic response. However, in practice, perfect sound diffusion is rarely achieved, requiring adjustments in some cases to account for furniture or surfaces not accounted for due to the assumption.

2.3 Measurement setup

Reverberation time measurements are conducted in accordance with the ISO 3382-2:2008 standard. Two microphone positions, M_1 and M_2 are marked within the room, spaced at least 1 [m] from the nearest reflecting wall, and avoids symmetric positions. Three sound source positions are utilized: two located at opposite corners of the room (S_1 and S_3) and one at the center, S_2 (see schematic in Fig. 1(b). The excitation signal is a time-domain logarithmic sine sweep, providing a high signal-to-noise ratio and enabling deconvolution to extract the room impulse response from which RT60 is estimated via Schroeder integration. The sweep is generated at –12 [dBFS] with a sampling rate of 44.1 [kHz].

A total of ${}^3P_2$ (= 6) source-microphone combinations were measured, and the results were averaged to obtain a single representative reverberation time curve. The office measurement setup comprises a Genelec 8020B active monitoring loudspeaker and an omnidirectional microphone, connected to the output and input channels, respectively, of a Focusrite Scarlett 2i4 audio interface. The measurement signals are generated and analyzed using Room EQ Wizard (REW) V5.31.3, allowing for precise estimation of the decay characteristics of the room impulse response.

3. RESULTS AND DISCUSSION

3.1 Model validation

Fig. 2 shows the one-third octave RT60 of the office space without any acoustic treatment. The measurements at each speaker-microphone position are shown in gray, while the average response is indicated in red (refer to Fig. 1(b) for speaker-microphone positioning). It is noteworthy that the office space was already in use, meaning some items could not be removed during measurements, which may have impacted the room's response. Subsequently, the numerical RT60 is compared to the experimental results. Initial simulation shows that the numerical model tends to overestimate the reverberation time. This discrepancy is likely due to the presence of surfaces, crevices, cavities, and other elements within the office space that are not fully accounted for in the numerical model. To correct for this, the unknown absorption characteristics are estimated by calculating the absorption area required to match the difference between the numerical and experimental RT60 responses. This "deficit" in absorption area is used to generate frequency-dependent absorption data, which are subsequently applied to a section of the room's wall in the numerical model. The required absorption area is computed using Sabine's equation as

$$\Delta A(f) = A_{exp}(f) - A_{num}(f) = \frac{0.161.V}{RT_{60}^{exp}} - \frac{0.161.V}{RT_{60}^{num}}, \tag{3}$$

So that the correction absorption coefficient, $\Delta\alpha(f)$, is then obtained according to Eqn. (4)

$$\Delta\alpha(f) = \frac{\Delta A(f)}{A_{corr}}, \tag{4}$$

where A_{corr} is the correction absorption area. The result of this correction is shown in Fig. 3 which validates the numerical for subsequent analysis.

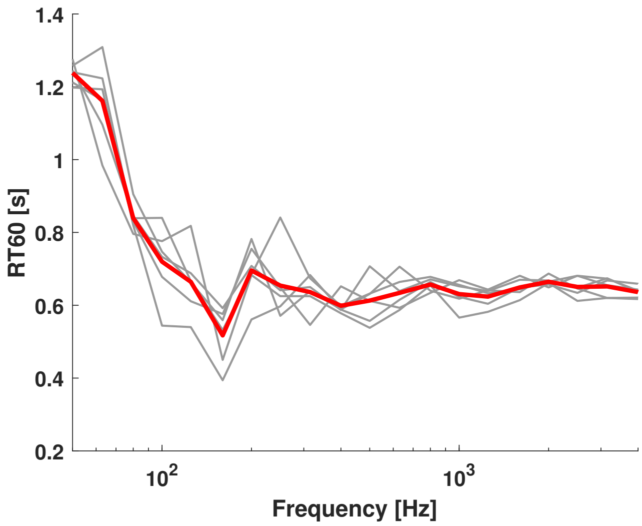

Figure 2: Acoustic response of the space measured using a logarithmic sine sweep excitation showing the reverberation time (RT60) and decay characteristics of the space.

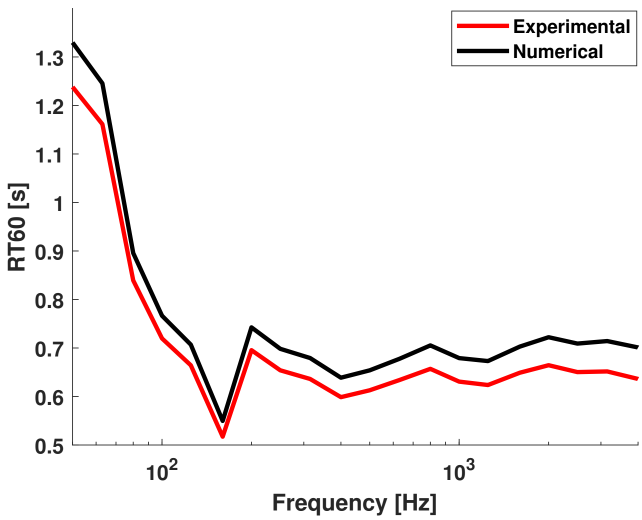

Figure 3: Comparison between experimental and numerical reverberation times after correcting for the unknown absorption area in the space.

3.2 AMM Application to Room Acoustics

Having validated the numerical room model against experimental measurements, a simulation study is conducted to evaluate the performance of a deep learning-based AMM absorber in comparison to a conventional industrial absorber, the Spektrum A10, which consists of a fabric cover and mineral wool core, with dimensions 60[cm] $\times$ 60 [cm] $\times$ 10 [cm]. A pre-trained autoencoder model is employed for inference, enabling the prediction of AMM geometrical parameters based on a desired target absorption spectrum. Here, the target spectrum is informed from the room's reverberation response in Fig. 2. The decoder component of the network is used to reconstruct the original input spectrum, which is subsequently applied to the AMM panels in the numerical room model. A unit structure of the designed AMM absorber is shown in Fig. 4. Each unit is a supercell composed of four inhomogeneous cells, each tuned to a different target frequency. The supercells are periodically arranged in a 60 [cm] $\times$ 60 [cm] rectangular panel, which is then applied to the room surfaces and ceiling. Four panels each of 60 [cm] $\times$ 60 [cm] cross-section are used in the simulation. On the other hand, the industry-grade Spektrum A10, shown in Fig. 5 is of similar cross-section, but witha thickness of 10 [cm]

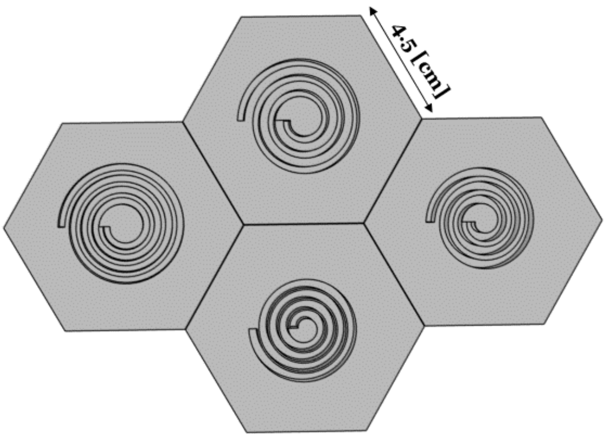

Figure 4: A unit structure of the designed broadband AMM absorber composed of a hexagonal cavity, a spiral inclusion and a top perforated plate.

For the private office space under consideration, it is desired to have RT60 between say $0.4 \leq$ RT60 ≤ 0.6 [s] at low frequencies ($<$ 200 [Hz]) to improve speech intelligibility and reduce listener fatigue from reflected noise. Thus, a broad range of 100 to 200 [Hz] with absorptivities higher than 0.8 is presented to the encoder for which the corresponding geometry is predicted, and the reconstructed absorption spectrum, $\alpha(f)$, is then applied to the

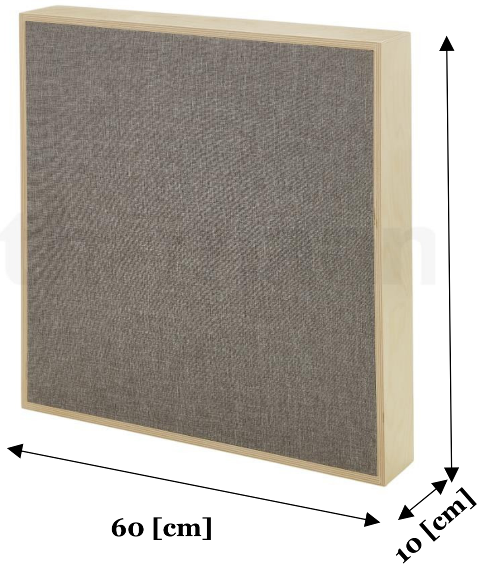

Figure 5: A 60 [cm] $\times$ 60 [cm] Spektrum A10 industrail panel used as a benchmark in this study

absorber surfaces in the room model. For fair comparison, the AMM absorber is also designed with the same 60[cm] $\times$ 60 [cm] cross-section, but with a thickness of 3 [cm]. Fig. 6 shows the performance comparisons of both absorbers. It can be observd that the AMM slighly improves the RT60 relative to the baseline in the range between 100 and 200 [Hz], but the effect at higher frequencies are very minimal. This is because the absorber is targeted for the low frequencies ($\leq$ 200 [Hz]) and more so, the range of influence of the aborber can be increased by increasing the number of inhomogeneous unit that makes up each broadband absorber, as low frequencies are characterized by sharp narrow peaks. The Spektrum A10 on the other hand performs better at higher frequencies ($>$ 200 [Hz]) with lower RT60. Fig. 7 shows a bar plot of the reduction in RT60 relative to the baseline. It is clear that the AMM provides a superior performance in the targeted low-frequency range, and beyond this range, the Spektrum A10 provides the better performance.

4. CONCLUSIONS

This paper presents a deep learning-driven acoustic metamaterial (AMM) absorber aimed at mitigating low-frequency room acoustic issues, and compares its performance with a conventional industry-grade absorber. The

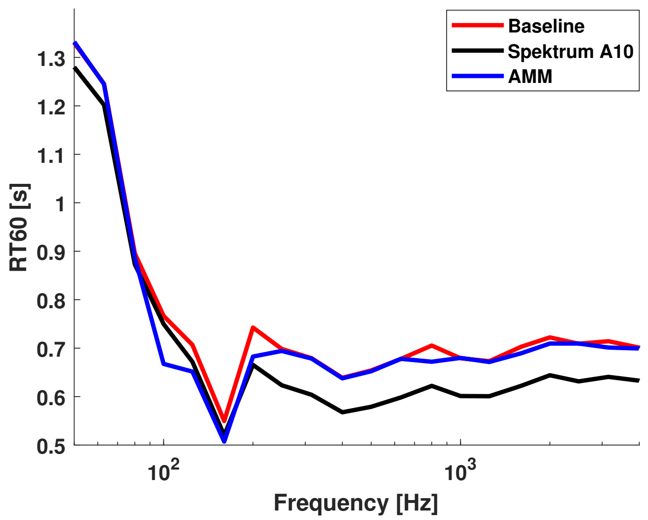

Figure 6: Performance comparison of RT60 curves from both absorbers relative to the baseline.

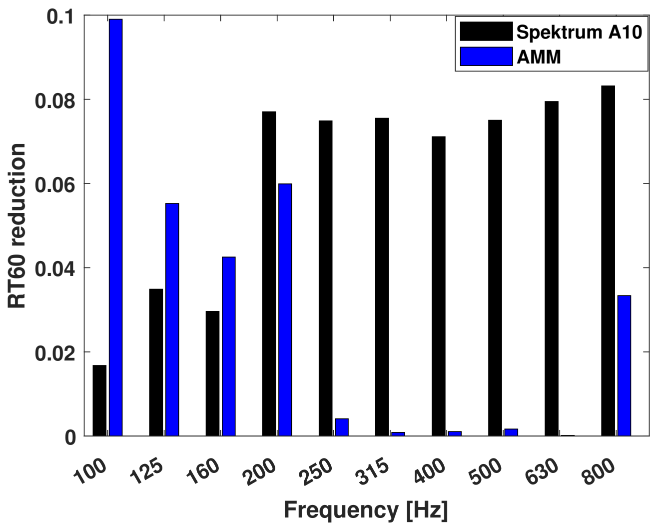

Figure 7: Relative difference in RT60 from the baseline from both absorbers in the targeted frequency range.

target environment is an existing office space that was partially evacuated and acoustically characterized using the RT60 metric.

To establish a baseline and validate the simulation framework, numerical modeling was carried out using the finite element method in COMSOL Multiphysics. Following validation, a pretrained autoencoder was employed to predict an optimal absorption spectrum in the 100–250 [Hz] frequency range. These frequency-dependent absorption coefficients were then applied to panel surfaces in the FEM model to simulate the corresponding reverberation times.

Simulation results demonstrate that the proposed AMM absorber shows promising performance within the targeted low-frequency range, with a modest reduction in RT60 compared to the untreated baseline response. However, the commercial Spektra A10 panel, with a thickness of 10 [cm], slightly outperforms the 3 [cm] thick AMM at higher frequencies above 200 [Hz]. This performance gap is primarily attributed to the limited number (four) of inhomogeneous unit cells used in constructing the broadband AMM absorber. It is anticipated that increasing the number of such units would broaden the effective bandwidth and enhance overall absorption performance over a wider operational range.

5. ACKNOWLEDGMENTS

The authors gratefully acknowledge the support of the Provost's awards of Trinity College Dublin.

6. REFERENCES

[1] L. Savioja and U. P. Svensson, "Overview of geometrical room acoustic modeling techniques," *The Journal of the Acoustical Society of America*, vol. 138, no. 2, pp. 708–730, 2015.

[2] H. Kuttruff, *Room acoustics*. Crc Press, 2016.

[3] M. Kleiner, B.-I. Dalenbäck, and P. Svensson, "Auralization-an overview," *Journal of the Audio Engineering Society*, vol. 41, no. 11, pp. 861–875, 1993.

[4] M. Vorländer, "Computer simulations in room acoustics: Concepts and uncertainties," *The Journal of the Acoustical Society of America*, vol. 133, no. 3, pp. 1203–1213, 2013.

[5] L. Aspöck and M. Vorländer, "Room geometry acquisition and processing methods for geometrical acoustics simulation models," *Proceedings of the EuroRegio*, 2016.

[6] A. Bassuet, D. Rife, and L. Dellatorre, "Computational and optimization design in geometric acoustics," *Building Acoustics*, vol. 21, no. 1, pp. 75–85, 2014.

[7] D. Murphy, M. Beeson, S. Shelley, A. Southern, and A. Moore, "Renderair – room acoustics simulation using a hybrid digital waveguide mesh," in *Proceedings of the 124th AES Convention*, (Amsterdam, The Netherlands), May 2008.

[8] K. Kowalczyk and M. van Walstijn, "Room acoustics simulation using 3-d compact explicit fdtd schemes," *IEEE Transactions on Audio, Speech, and Language Processing*, vol. 19, no. 1, pp. 34–46, 2011.

[9] K. Yee, "Numerical solution of initial boundary value problems involving maxwell's equations in isotropic media," *IEEE Transactions on antennas and propagation*, vol. 14, no. 3, pp. 302–307, 1966.

[10] E. Trocka-Leszczynska and J. Jablonska, "Contemporary architectural design of offices in respect of acoustics," *Applied Acoustics*, vol. 171, p. 107541, 2021.

[11] J. Keränen, P. Virjonen, D. Oliva Elorza, and O. V. Hongisto, "Design of room acoustics for open offices," *SJWEH Supplements*, no. 4, pp. 46–49, 2008.

[12] A. AlOmani, K. El-Rayes, and A. Altuwaim, "Optimizing the use of acoustic materials in office buildings," *Scientific reports*, vol. 11, no. 1, p. 20652, 2021.

[13] H. Fuchs, X. Zha, X. Zhou, and H. Drotleff, "Creating low-noise environments in communication rooms," *Applied Acoustics*, vol. 62, no. 12, pp. 1375–1396, 2001.

[14] R. Falcon Perez, "Machine-learning-based estimation of room acoustic parameters," 2018.

[15] G. Ciaburro and G. Iannace, "Acoustic characterization of rooms using reverberation time estimation based on supervised learning algorithm," *Applied Sciences*, vol. 11, no. 4, p. 1661, 2021.

[16] M. J. Crocker, F. M. Kessler, and A. J. Price, *Noise and Noise Control: Volume 1*. Crc Press, 2018.

[17] P. Jensen, C. R. Jokel, and L. N. Miller, "Industrial noise control manual," 1978.

[18] T. Rossing, *Springer handbook of acoustics*. Springer Science & Business Media, 2007.

[19] L. L. Beranek, "The notebooks of wallace c. sabine," *The Journal of the Acoustical Society of America*, vol. 61, no. 3, pp. 629–639, 1977.